Structural performance of half scissor-like elements deployable structure

Teck Jung Chai[1], *Cher Siang* Tan[2*] and *Shahrin* Mohammad[2]

[1]Department of Civil Engineering, Politeknik Sultan Idris Shah, Sungai Lang, 45100 Sungai Ayer Tawar, Selangor, Malaysia.
[2]School of Civil Engineering, Faculty of Engineering, Universiti Teknologi Malaysia, 81310 UTM Skudai, Johor, Malaysia.

Abstract. An experimental investigation on the Half Scissor-Like Elements (H-SLEs) mechanism deployable structure under compression axial load is presented. Two prefab cylindrical shape H-SLEs mechanism deployable steel structures namely M1 (Bolted base column) and model M2 (Unbolted base column) were tested on their performance in term of strength and stability performance. The model prototype consists cold-formed and hot roll steel with bolted connection and tested at deployed vertical configuration. Compression axial load was applied at the middle top of loading platform, transferred equally to the six H-SLEs deployable mechanism through supporting beams. The experimental results obtained indicated that three types of failure modes, i.e. excessive bearing capacity failure at lipped C-section flange around bolt hole perimeter, instability due to horizontal displacement at mid-height of H-SLEs deployable mechanism (Bolted joint area) and member buckling. Among these failures, horizontal displacement nominated the overall structure stability while section thickness impacts member bucking and bearing capacity. The experimental ultimate load was 1.63% greater than BS EN 1993 design load resistance for M1 condition while 30% less for M2 condition. The applied load difference between these two model prototypes was 31.15%. Thus, M1 ultimate loads capacity was satisfactory since less than 15% acceptable level while M2 not satisfactory. Beside, horizontal displacement was identify highly impacted scissor mechanism deployable structure instability and suitable member thickness may avoid section premature failure.

1 Introduction

Scissor-Like Elements (SLEs) mechanism deployable structures was widely used in various fields of technical application including civil engineering [1] since first established in year 1961 [2]. This structure behave as mechanism during deployment and load bearing at final deployed configuration [3]. The basic SLEs mechanism deployable structure is showed in Fig. 1 [4]. Todays, fast build modular unit volume becomes increasingly large and storage launching space at vehicle is limited has trigger inventors to adopt transformable technique

* Corresponding author: tcsiang@utm.my

with compact size during manufacturer and stably extended as designated geometry at site [5] to achieve productivity. Therefore, SLEs mechanism deployable structures come to place with innovative design and friendly system has become a famous topic recently.

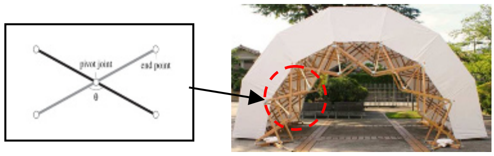

Fig. 1. Scissor-like elements (SLEs) mechanism for deployable structure application [4].

Previously, many studies have been conducted to explore the structural performance of SLEs mechanism deployable structure at fully deployed state. These research conducted tends to identify and solve the problems such as stabilization at deployed configuration [2], catastrophic failures [6], snap through effect problem [6], deployment issue [7], perimeter inconsistency [8], system stability [9] and foldability of translational, cylindrical and spherical configurations [10]. According to Andrea et al, the applications of space deployable structures main challenge remains to ensure high reliability in deployed geometry, stiffness and their function [11]. Li et al (2017) has examined SLEs column stability under gravity load using energy theory [12]. Roovers and De Temmerman (2017) has proposed the design methods and alignment concept to develop SLEs deployable structures [13]. Zhao et al (2020) has identified bending moment and pivot endpoints position adjustment to improve self-locking capability for SLEs structure through experimental and numerical studies [14].

The recent SLEs mechanism deployable structure research has focused on their deployment stage performance [3] but lack studied conducted on deployed stability [15]. There are few experimental studies carried out on SLEs mechanism deployable structures instability since it can suddenly bow with large lateral displacement under compression axial load and finally, member fail in bucking [16]. The structural performance instability has already attracted wide attention of researchers since the elastic curve and buckling load of slender column were developed by Euler [12]. According to Raskin and Roorda, column axial stiffness was greatly increased and snap-through buckling effect postponed under compression load with additional restraint [17]. The number of scissor units and degree of deployment must be counted for structure instability measurement [18]. In 2017, Li et al has successfully determined the SLEs deployable structure instability under its own weight using analytical method [12]. The SLEs mechanism deployable structure must able to bear external loads at deployed configuration [19]. Structures instability may have deformed and destroyed the deployable structure when service loads exceeded critical value, even not reached yield limit [20].

Thus, this paper establishes a novel experimental work to investigate the structural instability of Half Scissor-Like Elements (H-SLEs) mechanism deployable structure under compression axial load. At the end of the experimental work, the critical parameters and failure modes impacts the structure instability were determined and discussed.

2 Section and geometry properties

The prefab H-SLEs mechanism deployable structures model prototype was constructed using cold-formed steel lipped C-section, rectangular hollow section (RHS), reinforcement bar and mild steel plate. The cylindrical shape H-SLEs mechanism deployable structures model prototype dimension is 1.7 m diameter and 1.2 m height. The cold-formed lipped C-section was used as H-SLEs deployable mechanism, RHS as roof beam, reinforcement bar as restraint ring beam and mild steel as loading platform and base. The section capacity used was calculated according to the Eurocode 3 Standard [21 – 23]. The actual average yield strengths found from tensile test were 550 MPa and 518 MPa for 0.75 mm and 1.6 mm thick cold-formed C-section, 551 MPa for 12 mm diameter rebar and 333 MPa for 3 mm thick RHS. Thus, the section capacity was designed using steel strength of 500 MPa for cold-formed steel and reinforcement bar while 275 MPa for RHS section to ensure quality assurance. The fasteners used in the study were bolt grade 8.8 with 10 mm diameter. The material and section properties are tabulated in Table 1.

Table 1. Section and material properties.

Specimen	t mm	A mm^2	I_z mm^4	I_y mm^4	W_y mm^3	W_z mm^3	f_y MPa	f_u MPa	E MPa
C 74×36×6	0.75	106.9	17286	93778	2718	743.7	550	591	97178.6
C100×50×12	1.6	332.5	110855	533401	11305	3540	518.3	571.2	100971
RHS 75×38	3	635.5	151925	453693	7948	11864.2	333	436	123225

Reinforcement Bar					
Specimen	**$\emptyset$ (mm)**	**A (mm^2)**	**f_y (MPa)**	**f_u (MPa)**	**E (MPa)**
Ribbed Bar	12	113.1	551	640	76449

3 Experimental work

3.1 Experimental configuration and apparatus setup

The H-SLEs mechanism deployable structure model prototype was setup at deployed configuration with apparatus and of Linear Variable Differential Transduces (LVDTs) and strain gauges (SGs) positions as showed in Fig. 2. Two same design and dimension model prototype were used namely M1 and M2. The difference between these two models is M1 H-SLEs mechanism to base connection was hinge with additional two numbers of grade 8.8 M10 bolt tighten while M2 hinge connection only. The bolted connection was used to connect top ends with loading platform while Y 12 ring beam locked into J-hook position at intermediate level. The H-SLEs mechanism deployable structure was investigated under compression axial load to examine their capability in sustaining load applied.

A total of 13 numbers LVDT were used to measure horizontal displacement (12 Nos, Fig. 2c) and vertical displacement (1 No). Besides, a total of 11 numbers of 6 mm gauge length 120 Ω SGs were stickled at intermediate level ring beam and six H-SLEs mechanism (Fig. 2c). The type of test arrangement employed in this study was the six H-SLEs mechanism will displaced horizontally either inward or outward direction due to compression axial load applied. The point load was applied at the middle top of 790 mm x 790 mm x 20 mm thick steel plate to distribute the point load equally to six H-SLEs mechanism. The restraint ring beam will have subjected to compression due to horizontal displacement at H-SLEs mechanism joint area caused by compression axial load. The hydraulic jet with 300 kN load cell was used to apply load (Fig. 2b).

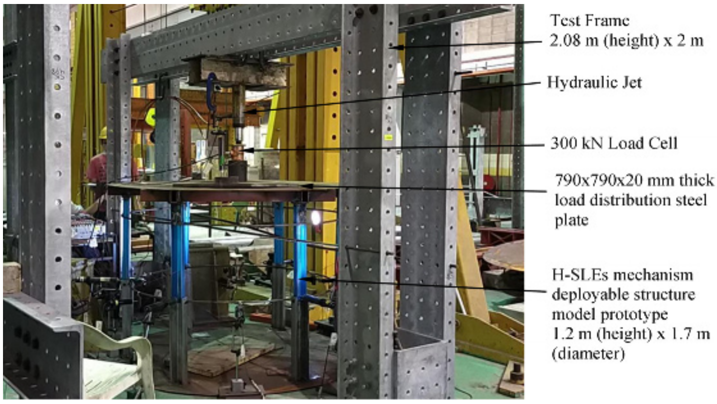

(a) Compression axial load test configuration

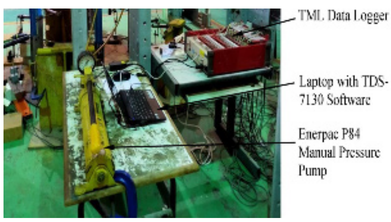

(b) Load test apparatus

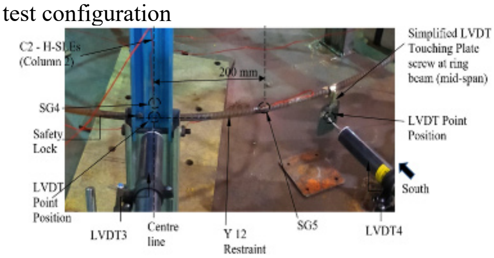

(c) LVDTs and SGs positions

Fig. 2. Load test configuration and apparatus setup.

3.2 Load test procedures

The initial compression axial load of 5 kN, which is approximately 10% of total maximum expected load was applied to the loading plate to ensure all joints fit and ready to apply loads. Then, the load cell was set back to initial zero to start the actual load test. The applied load was 1 kN/ step manually using hydraulic jet and the loads apply were leave for at least 60 seconds and onwards to obtain the static load. This step was repeated until the structure failed. During load test, the observation also carried out to identify the failure modes occurred to the members and joints. Besides, the first started and further failure point and mode of failure also identify along the load test. The parameters such as maximum load, horizontal displacements, member strain, member buckling and bearing capacity were determined and recorded. The raw data of the load test were recorded in the TDS-7130 software and then analysed for discussion and finding.

4 Results and discussion

The experimental data obtained was presented in graph and table and the observation results such as failure modes throughout the test was identified and discussed (Fig. 3). The summary of compression axial load test results for M1 and M2 were tabulated in Table 2. The results obtained indicated that excessive bearing deformation first observed at C1 bolt hole perimeter area (C74 flange), follow by C4 for M1. The similar failure also observed for M2 at C5, follow by C2. Both models H-SLEs mechanism showed the same horizontal movement direction during each element failed. For example, C1 and C5 displaced horizontally outward direction (-ve) while C4 and C2 horizontally inward direction (+ve). This scenes become more obvious with the increment of loads and when reached ultimate load at 59.74 kN (M1) and 41.13 kN (M2), all C74 section suffered from similar failures.

Besides, buckled failure mode also observed at the thin C-section flange and lipped area due to horizontal movement of the H-SLEs mechanism at joint area either inward or outward direction and caused push and pull effect. The top end node plate of H-SLEs mechanism also deformed (Fig. 3 ii) at failed column C4 (M1) and C2 (M2) due to shortening effect pulled the member C4 (M1) and C2 (M2) downward and the H-SLEs mechanism moved horizontal inward direction.

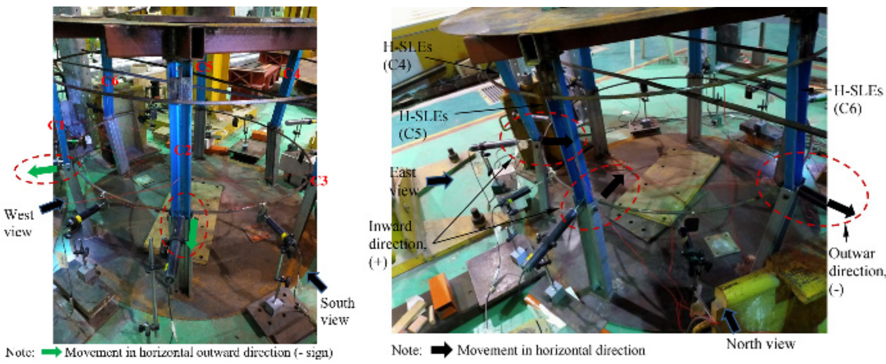

(i) Model prototype failure views

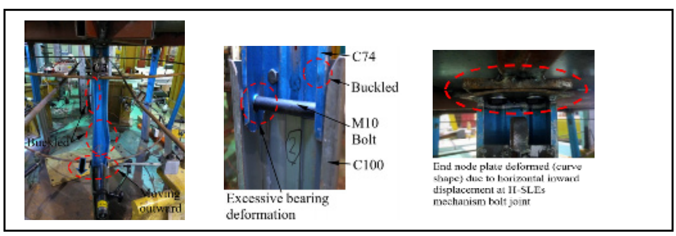

(ii) Failure modes observed

Fig. 3. H-SLEs deployable structure failure under compression axial load test.

Table 2. Summary of compression axial load test results.

<table>
<tr><th rowspan="2">Model Id</th><th rowspan="2">Applied Load (kN)</th><th rowspan="2">BS EN 1993 Design Load(kN)</th><th rowspan="2">Applied/ Predic-td Ratio</th><th rowspan="2">% Dif. Applied Load M1 & M2</th><th colspan="2">Horizontal Disp. (mm)</th><th rowspan="2" colspan="2">Failure Mode</th></tr>
<tr><th>+ ve</th><th>-ve</th></tr>
<tr><td>M1</td><td>59.74</td><td>58.78</td><td>1.02</td><td rowspan="2">31.15</td><td>46.7</td><td>26.3</td><td rowspan="2" colspan="2">Excessive Horizontal Displacement</td></tr>
<tr><td>M2</td><td>41.13</td><td>58.78</td><td>0.70</td><td>6.1</td><td>23.1</td></tr>
<tr><td colspan="9">Cold-Formed C-Section Capacity For H-SLEs Mechanism (Column)</td></tr>
<tr><td rowspan="2">Model Id</td><td colspan="2">Load (kN)</td><td colspan="3">Horizontal Disp. (mm)</td><td colspan="2" rowspan="2">Failure Mode</td><td rowspan="2">Remark</td></tr>
<tr><td>C1</td><td>C4</td><td>C1</td><td colspan="2">C4</td></tr>
<tr><td>M1</td><td>32.36</td><td>46.71</td><td>- 5.39</td><td colspan="2">+ 8.93</td><td colspan="2" rowspan="3">Excessive bearing deformation at flange bolt hole perimeter</td><td rowspan="3">C = Column</td></tr>
<tr><td rowspan="2">M2</td><td>C5</td><td>C2</td><td>C5</td><td colspan="2">C2</td></tr>
<tr><td>16.90</td><td>31.25</td><td>- 5.45</td><td colspan="2">+ 2.04</td></tr>
</table>

Based on the results obtained in Table 2, the actual ultimate loads for M1 was greater than BS EN 1993 design load resistance while M2 was less. This happened due to the M1 H-SLEs mechanism to base connection was hinge with additional M10 bolt tighten. The

M1 ultimate load obtained was satisfactory since less than 15% acceptable level but M2 result was not satisfactory. Thus, further discussion for the result analysis will focused on M1 only. Besides, the horizontal displacement inward direction was almost two times the horizontal displacement outward direction value when reached the model ultimate load capacity for M1.

The load versus horizontal displacement results for six H-SLEs mechanism indicated that Column 1, 2, 3 and 6 displaced horizontally outward direction (-ve) while Column 4 and 5 displaced horizontally inward direction (+ve) as showed in Fig. 4. The horizontal inward direction movement was greater than outward direction movement. The load-displacement curve obtained showed the similar pattern except failed column C4 after load 53.93 kN. Besides, the adjacent H-SLEs mechanism such as C3, C5 and C6 also indirectly impacted by C4 such as twisted and buckled due to pull and push effect (Fig. 3ii). Similar curve pattern for C1 and C4 from initial 0 kN to 50 kN happened may be due to these two columns have suffered early excessive bearing deformation at flange bolt holes perimeter. The slope line with big steepness in between two points load (Between 50.28 kN to 53.93 kN) will have a weak connection since the displacement value is high. This may enable the H-SLEs mechanism to move easily either inward or outward horizontal direction without resistance. For example, the smallest slope value obtained was 1.18 for C4 compared with C3 (1.31), C6 (3.65), C1 (5.53), C2 (6.08) and C5 (12.17). This indicated that the weakest H-SLEs mechanism in resisting horizontal displacement was C4 and vice-versa was C5. Thus, the horizontal displacement values obtained may represented the strongest or weakest of H-SLEs mechanism in resisting compression axial load applied.

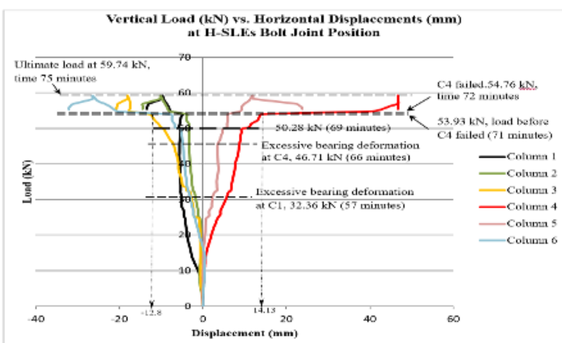

Fig. 4. Load versus displacements for H-SLEs mechanism.

The load versus displacement at restraint ring beam mid-span (Between two H-SLEs mechanism) was presented in Fig. 5. The restraint ring beam behaviour between two columns, C3 to C4 (RB/C3-4) and C4 to C5 (RB/C4-5) have a radial displacement outward (+ve) at mid-span while the others showed the radial displacement inward (-ve) at mid-span between two columns. The RB/C3-4 and RB/C4-5 displaced radially outward aims to balance the inward horizontal displacement at H-SLEs mechanism C4. Besides, the H-SLEs mechanism between C5 and C6 (RB/C5-6) indicated the radial displacement direction was changed from outward 0.03 mm to inward -0.03 mm at load 19.95 kN.

The load-displacement value for RB/C5-6 was up to the maximum load of 57.74 kN with radial displacement inward of -18.27 mm and beyond the load of 57.74 kN, the LVDT 10 was out of touching point. The RB/C4-5 at LVDT 8 position was also out of LVDT touching point at maximum load 54.76 kN with radial displacement inward of -23.04 mm. This scenario happened was due to the H-SLEs mechanism C4 displaced inward horizontally and failed. The radial displacement for restraint ring beam at load 19.95 kN and onwards has play the role to balance the horizontal displacements at H-SLEs

 https://doi.org/10.1051/e3sconf/202234701005

mechanism. This was because restraint ring beam produced two radial outward displacements and four radial inward displacements while for H-SLEs mechanism, it was two horizontal inward displacements and four outward displacements.

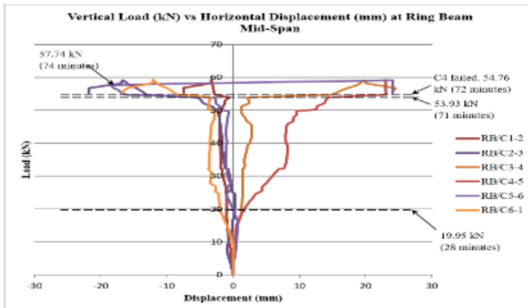

Fig. 5. Load versus displacements for restraint ring beam.

The members strain under compression axial load test was showed in Fig. 6. Based on the result obtained in Fig. 6(a), all the H-SLEs mechanism were under compression from initial load represent the linear relationship between load and strain except C4 have changed their trend towards tension strain direction after load 20.54 kN. During excessive bearing deformation occurred at C4 (Member C74) during load 32.36 kN, the tension strain value measured was 20 μe (4.2 N/mm^2). But when the load exceeds 54.76 kN, the further increment of load has caused the compressive strain at C5 moving towards tension strain. The changes of compressive strain to tension strain has caused the H-SLEs mechanism (C4) suffered excessive displacement and failed at load 54.76 kN while others H-SLEs mechanism (C1, C2, C3 and C6) show the vice-versa scenario with C4 and C5 condition. The C6 was the most stress H-SLEs mechanism under compressive strain (-ve, shortening) while only C4 at tensile strain (+ve, elongation). In this experiment, all six H-SLEs mechanism were projected under compressive stress but C4 changed from compressive to tension stress has caused the structure failed. Thus, the H-SLEs mechanism deployable structure must possess same types of stress or direction occurred during same time period to avoid failure.

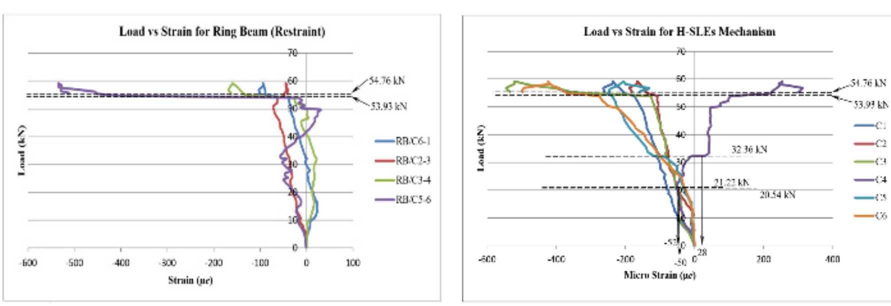

(a) H-SLEs mechanism (Column) (b) Intermediate level restraint ring beam

Fig. 6. Load versus strain.

The load versus strain at mid-span between two H-SLEs mechanism at intermediate level restraint ring beam was showed in Fig. 6(b). The results obtained indicated that the restraint ring beam was under compressive stress and section between C5 and C6 was the most stress section and follow by C3 and C4 section compared with others at load 54.76 kN. All these two ring beam section were adjacent to failed H-SLEs mechanism C4.

Apparently, it can be concluded that the restraint ring beam was under compression due to compression axial load and differ internal member stress may cause failure to H-SLEs mechanism.

5 Conclusion

An experimental study was conducted to investigate the H-SLEs mechanism deployable structures performance under compression axial load. The finding indicated that horizontal displacement dominated structures instability while section thickness impacts member buckling and bearing capacity. The load-displacement slope line with big steepness in between two points load will have a weak connection since the displacement value was high and vice-versa. The same type of internal member stress will maintain model stability and opposite stress will caused failure. Besides, two radial displacements from restraint ring beam was required to balance one inward displacement from H-SLEs mechanism. The actual ultimate loads for M1 was performed closely and greater than BS EN 1993-1-1 and BS EN 1993-1-3 design load resistance with the ratio of 1.02 while M2 was less with ratio of 0.7. The ultimate load capacity difference between M1 and M2 was 31.15 %. The M1 ultimate loads values obtained was satisfactory since less than 15% acceptable level but M2 result was not satisfactory where 15% acceptable level exceeded. Therefore, future research for M1 condition is recomended to obtain the conclusive findings.

This work was supported by the Ministry of Higher Education under Fundamental Research Grant Scheme (FRGS/1/2020/TK0/UTM/01/7) and Universiti Teknologi Malaysia (UTM-FR 21H68).

References

1. G. Wojciech, P. Jan, S. Paulina. Proc. Eng. E **91**, 6 (2014)
2. R. A. Esther, Deployable Structures (Laurence King Publishing Ltd, UK, 2015)
3. Y. Chen, Design of structural mechanism (Uni. Oxford, New York, 2003)
4. H. Tagawa, N. Sugiura, S. Kodoma. IABSE Symp. Report (2015)
5. T. J. Chai, C. S. Tan. Int. J Psy. Rehab. E **24**, 17 (2020)
6. N. Friedman, A. Ibrahimbegovic. YBL J Built Env. E **1**, 18 (2013)
7. A. Kwan, Z. You, S. Pellegrino. Int. J Sp Str. E **8**, 11 (1993)
8. Z. You, S. Pellegrino. Int. J Solids & Str. E **34**, 22 (1997)
9. C. Gantes, J. C. Jerome, D. L. Robert, R. Yechiel. Comp. & Str. E **32**, 8 (1989)
10. T. Langbecker. Int. J Sp Str. E **14**, 15 (1999)
11. E. D. G. Andrea, B. Paolo. Adv. Sci. & Tech. E **83**, 9 (2013)
12. B. Li, S. M. Wang, C. J. Zhi, X. Z. Xue, M. Viliam. Mech. Sys. & Sig. Pro. E **83**, 5 (2017)
13. K. Roovers, N. D. Temmerman. Int. J Solids & Str. E **121**, 16 (2017)
14. Z. W. Zhao, W. B. Hu, L. Yu. Adv. Str. Eng. 13 (2020)
15. L. I. W. Arnouts, T. J. Massart, N. D. Temmerman, P. Z. Berke. Eng. Str. E **177**, 11 (2018)
16. T. H. G. Megson, Structural and stress analysis (Elsevier Ltd, UK, 2005)
17. I. Raskin, J. Roorda. J Eng. Mech. E **125**, 4 (1999)
18. B. Li, S.M. Wang, R. Yuan. J Hrb. Inst.Tech. E **46**, 5 (2014)
19. H.Y. Hu, Q. Tian, W. Zhang, D. Jin, G. Hu, Y. Song. Adv. Mech. E **43**, 24 (2013)
20. C.J. Gantes. Int. J Sp Str. E **15**, 21 (2000)
21. British Standard Institution. BS EN 1993-1-1: Design of steel structures - General rules and rules for buildings (2005)

22. British Standard Institution. BS EN 1993-1-3: Design of steel structures - Supplementary rules for cold-formed members and sheeting (2006)
23. British Standard Institution. BS EN 1993 - 1 – 8: Design of steel structures: Design of joints (2005)